The Plant Cell, Vol. 15, 119–132, January 2003, www.plantcell.org © 2002 American Society of Plant Biologists

AtATM Is Essential for Meiosis and the Somatic Response to DNA Damage in Plants[W]

Valérie Garcia,[a] Hugues Bruchet,[a] Delphine Camescasse,[a] Fabienne Granier,[b] David Bouchez,[b] and Alain Tissier[a,1]

[a] Laboratoire de Radiobiologie Végétale, Département d'Ecophysiologie Végétale et de Microbiologie, Commissariat à l'Energie Atomique, 13108 St. Paul-lez-Durance Cedex, France

[b] Laboratoire de Biologie Cellulaire, Institut National de la Recherche Agronomique, Route de Saint Cyr, 78026 Versailles Cedex, France

In contrast to yeast or mammalian cells, little is known about the signaling responses to DNA damage in plants. We previously characterized *AtATM*, an Arabidopsis homolog of the human ATM gene, which is mutated in ataxia telangiectasia, a chromosome instability disorder. The Atm protein is a protein kinase whose activity is induced by DNA damage, particularly DNA double-strand breaks. The phosphorylation targets of Atm include proteins involved in DNA repair, cell cycle control, and apoptosis. Here, we describe the isolation and functional characterization of two Arabidopsis mutants carrying a T-DNA insertion in *AtATM*. Arabidopsis *atm* mutants are hypersensitive to γ-radiation and methylmethane sulfonate but not to UV-B light. In correlation with the radiation sensitivity, *atm* mutants failed to induce the transcription of genes involved in the repair and/or detection of DNA breaks upon irradiation. In addition, *atm* mutants are partially sterile, and we show that this effect is attributable to abundant chromosomal fragmentation during meiosis. Interestingly, the transcription of DNA recombination genes during meiosis was not dependent on *AtATM*, and meiotic recombination occurred at the same rate as in wild-type plants, raising questions about the function of AtAtm during meiosis in plants. Our results demonstrate that *AtATM* plays a central role in the response to both stress-induced and developmentally programmed DNA damage.

INTRODUCTION

DNA Double-strand breaks (DSBs) present a serious threat to genomic integrity, and cells have evolved a variety of mechanisms to respond to this type of aggression. DSBs may occur as a consequence of cellular metabolism [e.g., during replication, after exposure to DNA-damaging agents, or as part of a developmentally regulated program such as meiosis V(D)J rearrangement (essential for lymphocyte development in mammals)]. Cellular responses to DSBs involve both tight control of cell cycle progression and the induction of DNA repair activities (Khanna and Jackson, 2001). Additionally, certain organisms, primarily multicellular animals, have evolved an apoptotic response to DSBs (Norbury and Hickson, 2001). DSBs can be repaired via two major routes: homologous recombination (HR) and nonhomologous end joining (NHEJ) (Karran, 2000). HR is conservative and requires the presence of an intact homologous DNA duplex. The choice to repair by HR or NHEJ is critical and depends on a variety of factors, such as the availability of an accessible homologous duplex and the position in the cell cycle. The complexity of this coordinated response—apoptosis, cell cycle arrest, induction of DNA repair activities, and choice of HR versus NHEJ—requires the presence of proteins whose role is to sense the damage, integrate the signals perceived, and signal to the appropriate effector proteins. The discovery of the human ATM gene, mutations which are responsible for the recessive autosomal chromosome instability disorder ataxia telangiectasia (AT), provided a candidate for these functions (Savitsky et al., 1995). The ATM protein is involved not only in DNA damage cell cycle checkpoints but also in the regulation of DNA repair activities and apoptosis (for review, see Kastan and Lim, 2000).

ATM belongs to a family of conserved eukaryotic proteins that have in common a C-terminal phosphatidylinositol 3-kinase domain, a more loosely conserved region upstream of the phosphatidylinositol 3-kinase domain called FAT (FRAP, ATM, TRRAP), and a conserved motif called FATC (FRAP, ATM, TRRAP, C terminus) at the very C terminus (Bosotti et al., 2000). Of this large family, the group that is involved in responses to DNA damage comprises two major divisions: the ATM and the ATR subgroups. There is now ample evidence

[1] To whom correspondence should be addressed. E-mail alain.tissier@cea.fr; fax 33-442-2526-25.

[W] Online version contains Web-only data.

Article, publication date, and citation information can be found at www.plantcell.org/cgi/doi/10.1105/tpc.006577.

that ATM responds specifically, as far as DNA damage is concerned, to DSBs, as judged from the sensitivity of cells from AT patients to ionizing but not to UV-B radiation (Xu and Baltimore, 1996; Rotman and Shiloh, 1998). On the other hand, ATR and related proteins such as Mec1p seem to be involved in the response to a different spectrum of DNA lesions (Kato and Ogawa, 1994; Cliby et al., 1998). ATM and ATR are believed to function via recognition of DNA damage (Smith et al., 1999; Andegeko et al., 2001) by an unknown mechanism and the stimulation of their kinase activities. ATM phosphorylates Ser or Thr residues in proteins but not in lipids (Kim et al., 1999). This activation of ATM triggers a phosphorylation cascade that taps into the regulatory circuit of the cell cycle, leading to arrest at various checkpoints (Zhou and Elledge, 2000). ATM also signals to DNA repair complexes, for example, via the phosphorylation of proteins such as BRCA1 (Cortez et al., 1999), NBS1 (Gatei et al., 2000), and c-ABL (Baskaran et al., 1997; Shafman et al., 1997), which in turn phosphorylates RAD51. These two responses, cell cycle control and regulation of DNA repair activities, are not completely independent, because mutations in DNA repair genes such as NBS1 also have an impact on cell cycle control (Jongmans et al., 1997). Thus, ATM, via its privileged position at the top of this complex regulatory network, is essential in triggering the appropriate DNA repair response, depending on the stage of the cell cycle, and conversely in arresting the cell cycle, depending on the extent and type of damage.

Plants are organisms for which this type of integrating factor would play a crucial role for several reasons. First, extensive genome plasticity is a hallmark of plants. Second, plant genomes often are replete with numerous duplications and repeated DNA, potentially the substrate for genome rearrangement (Blanc et al., 2000; Vision et al., 2000). Third, by their fixed mode of life, plants are exposed continually to environmental stresses (Rozema et al., 1997; Ries et al., 2000). To shed additional light on these peculiarities of plants with regard to the response to DNA breaks, we performed a functional study of an Arabidopsis ATM homolog, which we described in a previous study (Garcia et al., 2000).

Here, we present the isolation and study of two Arabidopsis mutants, each carrying a disrupting T-DNA insertion in *AtATM*. Our results suggest that AtAtm plays an essential role in the response to DNA damage in somatic cells as well as during meiosis.

RESULTS

Isolation and Molecular Characterization of *AtATM* T-DNA Insertion Mutants

To probe the in planta function of the *AtATM* gene, we searched for mutants using a reverse-genetics approach. Three collections of insertion mutants were screened: the *En/Spm* transposon insertion library from the Sainsbury Laboratory (Norwich, UK) (Tissier et al., 1999), the Institut National de la Recherche Agronomique (Versailles, France) collection of T-DNA (Bouchez and Hofte, 1998), and the Salk Institute T-DNA express database (La Jolla, CA). A single line carrying an insertion in the 3′ end of the gene was isolated from the Institut National de la Recherche Agronomique collection, and the corresponding allele was named *atm-1*. A second T-DNA insertion, giving the *atm-2* allele, was found in the Salk Institute T-DNA Express database. The *AtATM*–T-DNA junctions were amplified and sequenced to determine the exact positions and structures of the insertions (Figure 1). In the *atm-1* allele, the T-DNA is inserted in exon 78, with intact right and left borders and a 23-bp deletion in the ATM sequence. In *atm-2*, the T-DNA is inserted in intron 64, with an intact left border and a truncated right border. The *atm-2* insertion appears to be more complex, with a loss of 4 bp of genomic DNA and the insertion of filler DNA from other regions of the genome on both sides of the T-DNA (Figure 1C). The *atm-1* and *atm-2* mutations are in the Wassilewskija and Columbia backgrounds, respectively.

Using a PCR genotyping assay, we were able to follow the transmission of the T-DNA insertions in the self-progeny of heterozygous plants. For *atm-1* and *atm-2*, respectively, 23 of 94 (24.5%) and 9 of 40 (22.5%) plants were homozygous for the T-DNA insertion, 52 of 94 (55.3%) and 22 of 40 (55%) were heterozygous, and 19 of 94 (20.2%) and 9 of 40 (22.5%) were homozygous wild type. Thus, both *AtATM*-T-DNA insertions behave as single Mendelian loci ($\chi^2 = 0.75$ for *atm-1* and 0.20 for *atm-2*). All of the homozygous mutant plants were partially sterile (see below), and all of the heterozygous and homozygous wild-type plants were fertile. Plants of all genotypes had normal vegetative development. DNA gel blot analysis showed that a single insertion is present in both lines (data not shown). Protein gel blots probed with a polyclonal antibody raised against the 180 C-terminal AtAtm amino acids revealed the presence of a high molecular mass polypeptide ($\sim$450 kD) in wild-type but not in *atm-1* mutant total protein extracts (Figure 1B).

atm Mutants Are Partially Sterile

We observed a partial sterility phenotype in the progeny of self-fertilized heterozygous *atm-1* and *atm-2* +/− individuals (Figures 2A to 2D; see also supplemental data online). Genetic analysis indicated that the partial sterility cosegregates strictly with the homozygous mutant genotype (see above). On average, homozygous *atm-1* and *atm-2* mutants produced 5.6 and 9.2 seeds per silique ($n = 20$), respectively, versus 60.6 and 55.1 ($n = 20$) in the corresponding wild-type plants. No apparent vegetative growth defect was observed in *atm-1* and *atm-2* plants (see Figure 5 and supplemental data online). However, they did flower more profusely and for a longer time than wild-type plants, a feature

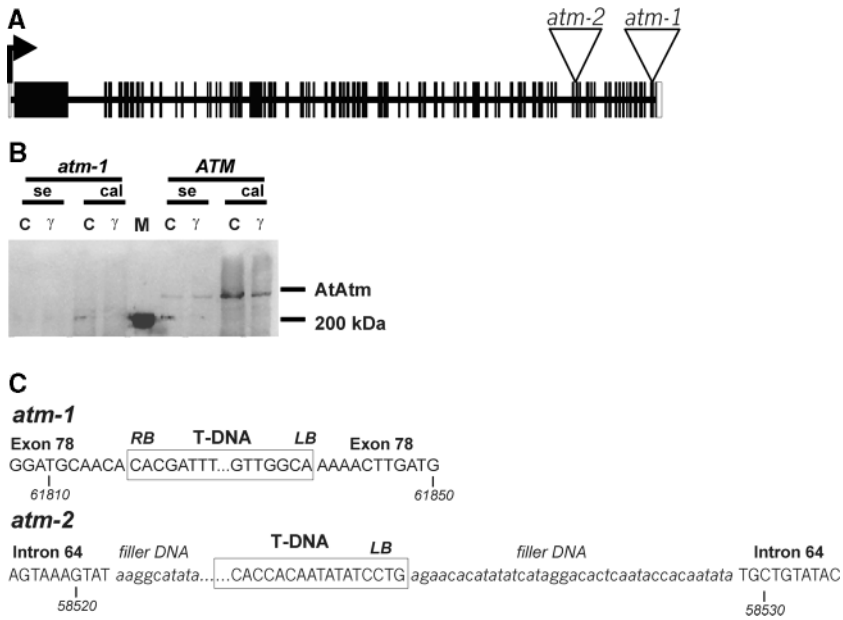

Figure 1. *AtATM* T-DNA Insertion Mutants.

(A) Genomic map showing the positions of the T-DNA insertions at the *AtATM* locus. The arrow indicates the transcriptional start site, and black rectangles represent exons. The triangles represent the T-DNAs inserted in intron 64 (*atm-2*) and exon 78 (*atm-1*).

(B) Protein gel blot analysis of the AtAtm protein with an anti-AtAtm specific polyclonal antibody in wild-type (ATM) and *atm-1* mutant calli (cal) and seedlings (se), both in the absence (C) and 1 h after γ-irradiation (γ; 100 Gy). The amounts of total protein loaded were 60 μg for seedlings and 250 μg for calli. M, molecular mass markers.

(C) Sequences of the *atm-1* and *atm-2* insertion sites. The T-DNA inserts are boxed. LB and RB indicate the left border and right border, respectively. Numbers below the sequence indicate the positions on the sequence of BAC T24C20. The right border of the T-DNA in *atm-2* could not be amplified with T-DNA primers. The junction was amplified by inverse PCR using primers on the genomic DNA. The *atm-2* T-DNA is accompanied by the insertion of filler DNA (lowercase italics) from other regions of the Arabidopsis genome.

typical of sterile mutants. Furthermore, seeds produced by both *atm* mutants were morphologically normal but slightly larger than those produced by the wild type (Figures 2E and 2F and data not shown). The average weight was 0.024 and 0.030 mg per seed for the *atm-1* and *atm-2* mutants, respectively, versus 0.015 and 0.026 mg per seed in the corresponding wild-type seeds (each estimated from the weight of 600 seeds). We noted the absence of abnormal seeds—dark, shrunken, and not viable—that have been observed commonly in other known sterile mutants of Arabidopsis (Couteau et al., 1999). The progeny of homozygous *atm-1* and *atm-2* mutants appeared indistinguishable from those of the parent plants, and the *atm-1* mutation was propagated over four generations without apparent phenotypic variation.

Gametophytic Development Is Arrested after Meiosis in the *atm-1* and *atm-2* Mutants

To determine the origin of the partial sterility of *atm* mutants, we first examined mature gametophytes in mutant plants. Because fertilization of *atm* pistils with wild-type pollen produced a low number of seeds, we checked for a defect in female gametophyte development. In wild-type ovules, only one of the four haploid megaspores survives and undergoes three rounds of nuclear division to form the embryo sac, which is the mature female gametophyte. Concomitant with embryo sac formation, surrounding tissues develop to form a curved mature ovule. Confocal laser scanning microscopy of flower buds stained according to Christensen et al. (1996) revealed that in the *atm-1* mutant, only 15.7% (31 of 197) of the functional megaspores divided and formed an embryo sac of two to eight nuclei, depending on the maturity of the silique observed. In the remaining ovules (84.3%), which apparently were mature (i.e., the teguments were fully developed and the ovules were curved), the functional megaspore did not divide and degenerated (Figures 3B and 3D). None of the ovules observed in the wild type showed arrest at early stages, as in the mutant, and all of the normal stages of ovule development were seen (Figures 3A and 3C).

Because the progeny of homozygous *atm-1* and *atm-2* mutants consists of 100% homozygous mutants, fertilization

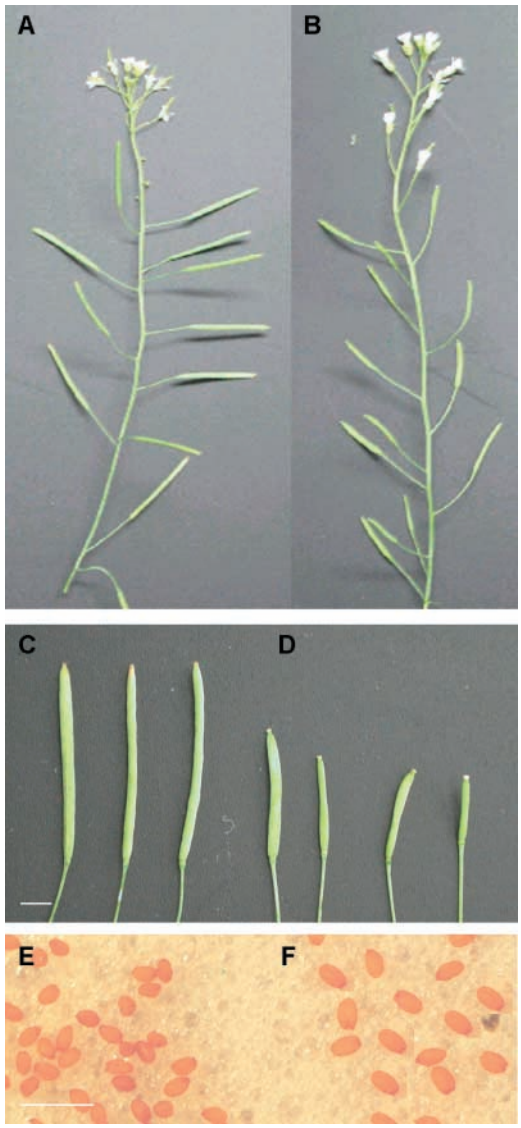

Figure 2. *atm-1* Mutants Are Partially Sterile.

Flowering stems (**[A]** and **[B]**) and siliques (**[C]** and **[D]**) of the wild type (**[A]** and **[C]**) and *atm-1* mutants (**[B]** and **[D]**) are shown. The siliques in the *atm-1* mutants are shorter than those in the wild type. Wild-type seeds **(E)** are reduced in size compared with *atm-1* seeds **(F)**. Bars = 1 cm for **(C)** and **(D)** and 1 mm for **(E)** and **(F)**.

of mutant embryo sacs must be achieved by mutant pollen grains. Staining of pollen grains according to Alexander (1969) showed that pollen grain viability was low in *atm-1* and *atm-2* mutants compared with the wild type (Figures 3E to 3H; see also supplemental data online). In *atm-1* and *atm-2* mutant anthers, the remaining viable pollen grains were morphologically normal. However, the reduced number of viable pollen grains was not limiting, because it was sufficient to fertilize a wild-type pistil upon outcrossing. Thus, the female gametophytic defect alone accounts for the observed partial sterility.

Meiosis Is Disrupted Severely in a Majority of *atm-1* and *atm-2* Meiocytes

To further define the cause of the sterility of the *atm-1* and *atm-2* mutants, and because Atm homologs in other organisms have been shown to play a role in meiosis (Carpenter, 1979; Kato and Ogawa, 1994; Lydall et al., 1996; Barlow et al., 1998), we searched for meiosis defects. Meiotic progression was monitored by 4′,6-diamidino-2-phenylindole (DAPI) staining of pollen mother cells from wild-type and *atm* mutant plants. Photographs demonstrating meiotic events from wild-type plants are shown in Figure 4. These meiotic events have been fully described previously (Ross et al., 1996). Prophase I is subdivided into five stages, from leptotene to diakinesis. The pachytene stage, characterized by full synapsis of homologous chromosomes, can be observed easily by DAPI staining (Figure 4A). This step is followed by the progressive condensation of the bivalents and the separation of the chromosomes, except at chiasmata (diakinesis; Figure 4B). At metaphase I, the five bivalents are condensed maximally and oriented on the spindle (Figure 4C). At anaphase I, the homologous chromosomes, each composed of two chromatids, migrate to opposite poles and then partially decondense (telophase I or "dyad"; Figure 4D). Individual chromosomes condense again and align on the metaphase II plate (Figure 4E). Individual chromatids then are separated and migrate to the cell poles during anaphase II (Figures 4F and 4G). Then, the four groups of five chromatids decondense, the cytoplasm is partitioned, and finally a tetrad of haploid nuclei is formed.

In the *atm-1* and *atm-2* mutants, chromosome pairing seems to occur as in wild-type plants during the pachytene stage (Figure 4H; see also supplemental data online). The absence of unpaired chromosomes, or univalents, during diakinesis or metaphase I in both *atm* mutants suggests that chromosome pairing takes place normally. This is based on the observation of 71 meiocytes at the metaphase I stage. However, in a fraction of *atm-1* and *atm-2* meiocytes, a number of anomalies were seen as early as diakinesis, including bridges between bivalents and lumping of two or more bivalents together (Figures 4I and 4J; see also supplemental data online). However, the most abundant and frequent anomaly is chromosome fragmentation, observed during anaphase I (Figures 4M to 4P; see also supplemental data online). Chromosome fragments, which are likely to be acentric, are excluded from the meiotic division spindle. Other fragments, possibly dicentric chromosomes, seem to remain attached to the spindle as if they were torn between the two groups of chromosomes. In addition, chromosome

bridges were observed during anaphase II (Figure 4Q; see also supplemental data online), suggesting that further fragmentation could occur during anaphase II as well. At the tetrad stage, several discrete DAPI-staining bodies, representing isolated fragments, are excluded from the four nuclei. Occasionally, these micronuclei are encapsulated by a cell wall, leading to the formation of polyads (Figure 4T; see also supplemental data online).

Apparent Meiotic Recombination Frequencies Are Normal in the *atm-1* Mutants

The presence of viable meiotic products allowed us to measure meiotic recombination frequencies using visible phenotypic markers, as described by Masson and Paszkowski (1997). Homozygous *atm-1* mutants were crossed with lines expressing phenotypic markers corresponding to linked recessive mutations (see Methods). For each cross, F2 plants heterozygous for the phenotypic markers and partially sterile (i.e., homozygous for the T-DNA insertion) or fertile (i.e., wild type or heterozygous for the T-DNA insertion) were selected. Recombination frequencies were estimated by counting the number of plants with parental and recombinant phenotypes in the F3 generation. No significant difference in the recombination frequencies was observed between *atm-1* and wild-type plants (Table 1).

Meiotic Recombination Genes Are Expressed at Normal Levels in *atm-1* Mutants

We quantified the expression of several meiosis-specific recombination genes (*AtRAD51*, *AtSPO11*, and *AtDMC1*) by real-time PCR in young inflorescences (see Methods). No significant difference was seen between *atm-1* and wild-type plants (Table 2). This analysis also showed that *AtRAD51* and *AtDMC1* are expressed at similar levels and at levels approximately fourfold higher than those of *AtSPO11*.

atm Mutants Are Hypersensitive to Ionizing Radiation and Methylmethane Sulfonate but Not to UV-B

To determine whether the *atm* mutations confer hypersensitivity to DNA-damaging treatments, wild-type and mutant 5-day-old seedlings were challenged with doses ranging from 20 to 200 Gray units (Gy) of γ-radiation. For doses ranging from 0 to 60 Gy, no difference was visible between mutant and wild-type plants (data not shown). For doses of 80 and 100 Gy, the *atm-1* and *atm-2* mutants clearly were more sensitive than the wild type. As shown in Figure 5A (see also supplemental data online), a 100-Gy irradiation resulted in necrotic cotyledons and developmental arrest. A 150-Gy irradiation induced lethality for both mutant and wild-type plants (data not shown). We also measured root elongation in the absence of and after irradiation (Figure 5B). Upon an irradiation dose of 80 Gy, root elongation decreased and was arrested permanently at day 3 after irradiation in the *atm-1* mutant, whereas the arrest was only transient in the wild type (Figure 5B).

Next, we tested the sensitivity of *atm-1* mutants to methylmethane sulfonate (MMS) at doses ranging from 0 to 100

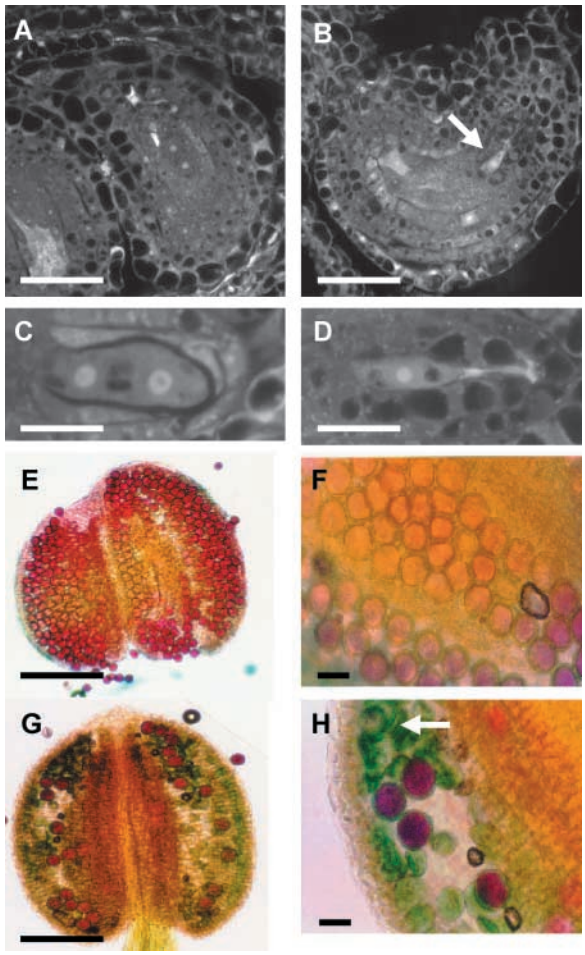

Figure 3. High Gametophytic Lethality in *atm-1* Mutants.

(A) to **(D)** Pistils were stained according to Christensen et al. (1996). Wild-type ovules show a normal development of embryo sacs **(A)**, whereas in *atm-1* mutants, the functional megaspore degenerates (**[B]** and **[D]**). Only a degenerate cell can be seen (arrow) in *atm-1* ovules, and no embryo sac has developed. Bars = 30 μm for **(A)** and **(B)** and 10 μm for **(C)** and **(D)**.

(E) to **(H)** Staining of mature anthers according to Alexander (1969). The pollen cell wall is stained green and the cytoplasm is stained pink, indicating viability. In the wild type (**[E]** and **[F]**), most pollen grains appear viable. In *atm-1* anthers (**[G]** and **[H]**), only a few pollen grains are viable, and the dead grains are green (arrow). Bars = 150 μm for **(E)** and **(G)** and 25 μm for **(F)** and **(H)**.

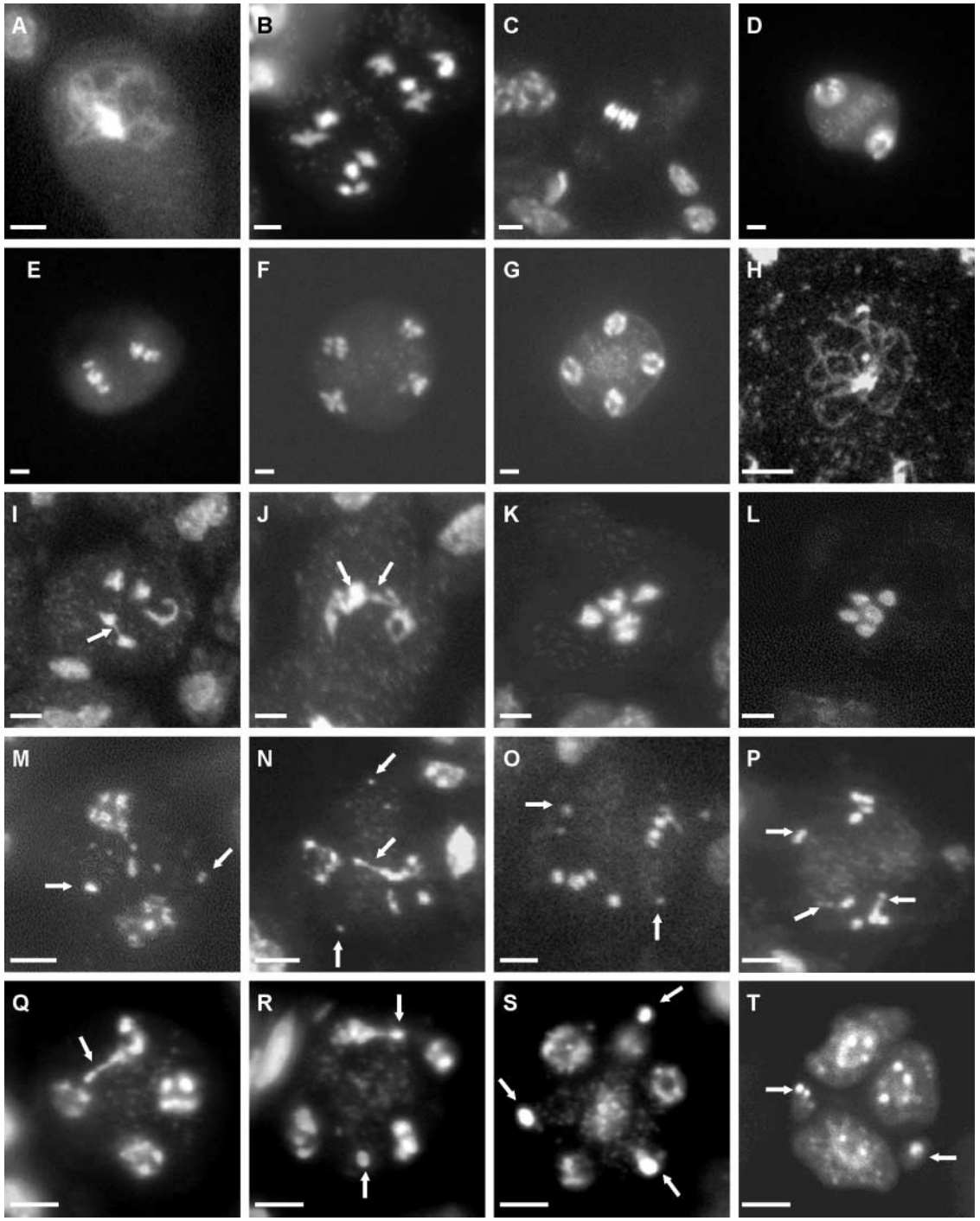

Figure 4. Meiosis in Wild-Type and *atm-1* Mutant Plants.

(A) to **(G)** Wild type.
(H) to **(T)** *atm-1*.
(A) and **(H)** Pachytene stage.
(B) and **(I)** to **(K)** Diakinesis.
(C) and **(L)** Metaphase I.
(D), **(M)**, and **(N)** Telophase I.
(E), **(O)**, and **(P)** Metaphase II.
(F), **(G)**, and **(Q)** to **(S)** Telophase II.
(T) A "polyad" with more than four microspores.
Anthers were stained with DAPI. Two juxtaposed nuclei are present in **(B)**. During anaphase/telophase I, chromosomal fragments are scattered through the pollen mother cells in the *atm-1* mutant. At the end of meiosis, extramicrosporial chromosomal fragments are visible outside of the four groups of chromosomes in the mutant tetrads. Arrows point to either bridges or abnormal chromosomal fragments. Bars = 10 μm.

Table 1. Meiotic Recombination Frequencies in the *atm-1* Mutant Are Normal

Genotypes Tested	Phenotypic Frequencies[a]				Meiotic Recombination Frequency (%)	χ^2
	P1	R1	R2	P2		
ATM/ATM; ch1-1 gl2-1/CH1 GL2	340	49	89	18	0.28	–[b]
atm-1/atm-1; ch1-1 gl2-1/CH1 GL2	170	33	35	18	0.26	7.47
ATM/ATM; ttg-1 yi-1/TTG YI	238	94	80	22	0.40	–
atm-1/atm-1; ttg-1 yi-1/TTG YI	399	123	106	24	0.35	4.72

[a] P1 and P2, parental phenotypes; R1 and R2, recombinant phenotypes.
[b] –, not applicable.

ppm (Figure 5C). MMS is an alkylating agent known to indirectly induce DSBs (Chlebowicz and Jachymczyk, 1979; Hryciw et al., 2002). A dose of 100 ppm was found previously to be sublethal for Arabidopsis seedlings of the Landsberg *erecta* type (Masson et al., 1997). After 15 days in liquid culture medium with doses of <50 ppm, the growth of wild-type and *atm-1* mutant plants was similar, whereas hypersensitivity was observed in the mutant at higher doses (50 and 60 ppm). For doses of 75 ppm or greater, lethality was induced within 15 days for both *atm-1* mutants and wild-type plants (data not shown). Thus, *atm-1* mutants also displayed enhanced sensitivity to MMS compared with wild-type plants.

Five-day-old seedlings were challenged with several doses of UV-B light (0 to 1 J/cm^2). The sensitivity was assayed by measuring root growth daily after the irradiation. For each tested dose, mutant seedlings behaved like the wild type, with no increase in sensitivity (data not shown).

The Transcriptional Induction of *AtRAD51*, *AtPARP1*, *AtGR1*Q7, and *AtLIG4* by Ionizing Radiation Is Defective in *atm-1* Mutants

In plants, ionizing radiation induces a strong, rapid, and transient transcriptional activation of genes involved in the cellular response to or repair of DSBs. These include *AtRAD51* (Klimyuk and Jones, 1997), *AtPARP1* (Doucet-Chabeaud et al., 2001), *ATGR1* (Deveaux et al., 2000), and *AtLIG4* (West et al., 2000). RAD51 is a eukaryotic homolog of RecA and is involved in the repair of DSBs by homologous recombination (Shinohara et al., 1992). PARP1 plays an important role in the recognition of DNA breaks and signaling to modulate other repair activities (Herceg and Wang, 2001). LIG4 is a DNA ligase associated specifically with NHEJ (Schar et al., 1997; Teo and Jackson, 1997; Wilson et al., 1997). The AtGR1 protein has homology with CtIP (Wong et al., 1998), a mammalian protein phosphorylated by ATM and associated with BRCA1 (Li et al., 2000), and is hypothesized to be involved in cell cycle regulation (Deveaux et al., 2000).

In the wild type, the *AtRAD51*, *AtGR1*, and *AtPARP1* basal levels of expression seemed to be very low, because we were unable to detect their transcripts by RNA gel blot hybridization (Figure 6). Within 30 min of irradiation, the signal corresponding to these transcripts increased rapidly and strongly, and it reached its maximal level between 30 min and 1 h after irradiation. This induction was transient, with a progressive reduction in the hybridization signals during the period observed (up to 6 h after irradiation). The expression profile of *AtLIG4* was different, with a moderate transient induction (twofold) and a maximum at 4 h after irradiation.

Interestingly, the transcriptional induction of *AtRAD51* was compromised severely in the *atm-1* and *atm-2* mutants, although there still was a very weak residual induction between 30 min and 2 h after irradiation (Figure 6). Similarly, no induction was seen in the cases of *AtPARP1* and *ATGR1*. For *AtLIG4*, the basal level remained unaltered compared with that in the wild type, but no induction was seen. The loss of transcriptional induction of *AtRAD51* and *AtLIG4* was confirmed in *atm-2* mutants by real-time reverse transcriptase–mediated PCR (see supplemental data online). Quantification of the transcripts also was performed in parallel on the *atm-1* mutants. This analysis showed that in the *atm-1* and *atm-2* mutants, there was a residual induction that amounted to ~10% of the wild-type level in the case of *AtRAD51*.

These results demonstrate that the Arabidopsis AtAtm protein plays a crucial role in the signaling that leads to the transcriptional response to ionizing radiation.

Table 2. Transcription of Meiosis-Specific Recombination Genes Is Normal in *atm-1* Mutants

Cycle Thresholds	18S	*AtRAD51*	*AtSPO11*	*AtDMC1*
Experiment 1[a]				
ATM	14.3	27.2	29.6	27.2
atm-1	14.6	27.4	29.4	27.5
Ratio *atm-1*:ATM		1.1	1.3	1.0
Experiment 2[a]				
ATM	13.6	27.7	29.9	28.2
atm-1	13.6	28.0	29.6	28.3
Ratio *atm-1*:ATM		0.8	1.2	1.1

[a] These correspond to independent RNA extractions.

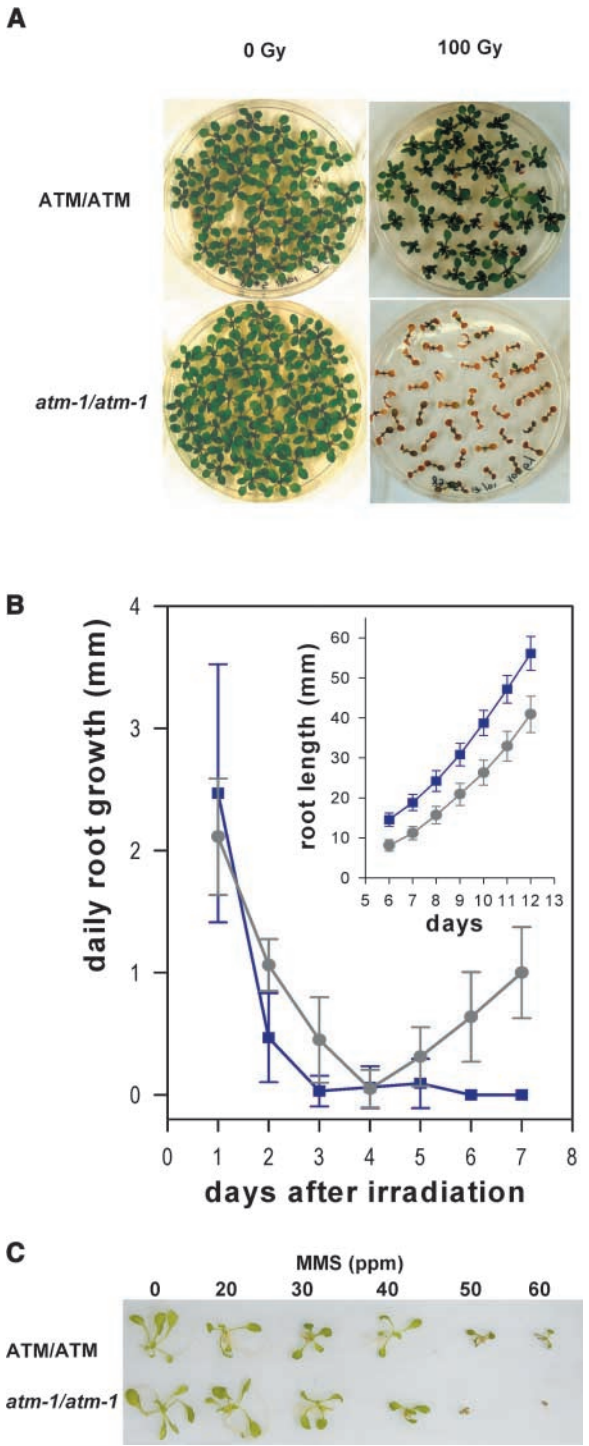

Figure 5. Hypersensitivity of the *atm-1* Mutants to γ-Rays and MMS.

(A) Wild-type (ATM/ATM) and mutant (*atm-1/atm-1*) 5-day-old seedlings were either left untreated (0 Gy) or subjected to 100 Gy of irradiation. The photographs were taken at 21 days after irradiation. The growth of wild-type plants has resumed (top right), whereas the growth of mutant seedlings is arrested (bottom right).

(B) Daily root growth after 80 Gy of irradiation of wild-type (gray circles) and *atm-1* (blue squares) 5-day-old seedlings. The inset shows a plot of the cumulative root growth in the absence of irradiation versus time (in days). *atm-1* mutant roots are ~30% longer than wild-type roots.

(C) Wild-type and *atm-1* 5-day-old seedlings were grown in the presence of the indicated concentrations of MMS (in ppm), and the photographs were taken on day 21.

DISCUSSION

We have isolated two *atm* mutants in Arabidopsis. Both insertions are located at the 3′ end of the gene, a region that encodes the phosphatidylinositol 3-kinase domain, which is essential for the activity of the Atm proteins (Rotman and Shiloh, 1998). Although in different ecotypes, both mutations give rise to identical phenotypes. The *atm-1* and *atm-2* mutations behave as single recessive markers. All of these observations strongly support the notion that the phenotypes observed in both mutants are the result of the loss of a functional AtAtm protein.

The Sterility of *atm* Mutants Is Caused by a Meiotic Defect

Cytological observation of male and female gametophytes in the *atm-1* and *atm-2* mutants indicated a low viability of the gametophytes, which resulted in partial sterility. Because heterozygous *atm-1* and *atm-2* +/− plants normally are fertile and the T-DNA insertion segregates in a Mendelian manner, a gametophyte-specific defect can be excluded. Thus, the low spore viability is attributable to earlier and sporophytic phases of gametogenesis (i.e., meiosis). Indeed, we found frequent aberrant meioses in *atm-1* and *atm-2* anthers, with extensive chromosome fragmentation leading to lethal consequences. Similarly, mutations in the *Saccharomyces cerevisiae MEC1* and *Drosophila melanogaster MEI-41* genes, as in mammalian *ATM*, lead to defects in meiosis (Carpenter, 1979; Kato and Ogawa, 1994; Lydall et al., 1996). The partial sterility phenotype of both *atm* mutants is consistent with an important role of AtAtm in meiosis and confirms a general conservation of the Atm meiotic function throughout eukaryotes. In the majority of *atm-1* and *atm-2* meiocytes, chromosome fragmentation was observed during anaphases I and II. As in the yeast *mec1* and Drosophila *mei-41* mutants, the meiotic defect did not affect the progression through meiosis in the Arabidopsis *atm-1* mutant. It is interesting that despite extensive chromosome fragmentation, Arabidopsis *atm-1* and *atm-2* meiocytes did not appear to undergo cell death before the end of meiosis. Thus, the high lethality among the *atm-1* and *atm-2* gametophyte populations presumably was the result of an aberrant

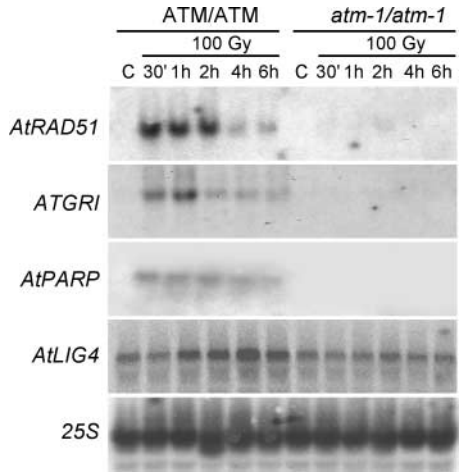

Figure 6. Transcriptional Activation of Genes Involved in the Cellular Response to DSBs Is Abolished or Delayed in *atm-1* Mutants.

Total RNA was extracted from 5-day-old seedlings untreated (C) or 30 min, 1 h, 2 h, 4 h, and 6 h after treatment with 100 Gy of irradiation. RNA gel blots (20 μg of total RNA per lane) were hybridized with probes from the *AtRAD51*, *AtPARP1*, *ATGR1*, and *AtLIG4* genes. Equal loading was checked by hybridization with a 25S ribosomal probe.

chromosomal content (aneuploidy and chromosome fragments). This finding underscores a major difference between plants and mammals, in which ATM deficiency results in early arrest in prophase I followed by apoptotic degeneration (Barlow et al., 1997). The absence of genes that code for a structural homolog of p53 or other proteins involved in apoptosis, such as BCL2 and caspases, in the Arabidopsis genome could account for this difference. Below, we discuss the possible causes of this fragmentation in the light of what is known in other Arabidopsis meiotic mutants and mutants in *ATM* homologs from other organisms.

Is There an *AtATM*-Dependent Meiotic Checkpoint in Arabidopsis?

The absence of meiotic arrest in *mec1* yeast, *mei-41* Drosophila, and *atm* mutants cannot necessarily be attributed to the absence of apoptosis, because at least in yeast, meiotic permanent arrest can occur without apoptosis induction. For example, some yeast *dmc1* strains are arrested during prophase I (Bishop et al., 1992), and this arrest depends on Mec1p activity (Lydall et al., 1996). Members of the Atm family are known for their role in the DNA damage cell cycle checkpoint during mitosis (Lydall and Weinert, 1995; Weinert, 1997). The suppression of *dmc1* arrest by *mec1* mutations was interpreted as an extension of this activity to the meiotic cell cycle (Lydall et al., 1996). Thus, the function of this meiotic, or pachytene, checkpoint would be to ensure that meiotic DSBs are repaired fully before chromosomes segregate. According to this model, a hypothesis to explain meiotic progression despite chromosome fragmentation would involve the loss of a pachytene checkpoint function in Arabidopsis *atm-1* mutants. In the absence of AtAtm, premature segregation before complete resolution of recombination intermediates would induce chromosomal disruption by pulling paired chromosomes toward the poles of the cell. However, in a fraction of the meiocytes, recombination intermediates would be resolved before the onset of anaphase I, and normal completion of meiosis would ensue.

However, the absence of permanent arrest in Arabidopsis *dmc1* mutants (Couteau et al., 1999) suggests the presence of a meiotic checkpoint in plants. Similarly, Arabidopsis meiotic mutants with not only asynapsis but also chromosomal fragmentation, such as *syn1* and *mcd1* (Ross et al., 1997), progress to the end of meiosis. If the function of AtAtm were to control meiotic progression, the anomalies that are present in those mutants would induce, through AtAtm, meiotic arrest. Thus, the question of the existence of a functional meiotic checkpoint in Arabidopsis remains open.

Another hypothesis to explain the presence of chromosome fragments involves inaccurate repair by homologous recombination. The meiotic recombination frequency in *atm-1* mutants, calculated from viable spores, was normal. Because this assay depends on spore viability to detect recombinant plants and viable spores have passed through a strong selection for euploidy, it is difficult to determine whether a homologous recombination defect might be the prime cause of abnormal meiosis. However, the facts that some spores are viable, and that we observed few normal meiotic figures by cytological analysis, suggest that if AtAtm is involved in homologous recombination during meiosis, its function is not essential. In addition, we observed that the expression of meiotic recombination genes (*AtRAD51*, *AtDMC1*, and *AtSPO11*) in *atm* mutants was normal. This finding suggests that the basic machinery for recombination is present in *atm* meiocytes and thus is in agreement with the normal levels of meiotic recombination in *atm-1* mutants. This result also suggests that if AtAtm modulates the activity of these genes during meiosis, it is likely to be at the post-transcriptional level, presumably via phosphorylation.

atm Plants Are Hypersensitive to Ionizing Radiation and MMS

In addition to their meiotic phenotype, *atm-1* plants are hypersensitive to ionizing radiation and MMS. Ionizing radiation induces a number of DNA lesions, including oxidative base damage, single-strand breaks, and DSBs (Thacker, 1999). The methylated bases produced by MMS are repaired by enzymes of the base excision repair pathway, producing abasic sites (Angelis et al., 2000). These abasic sites inhibit DNA replication and are presumed to cause DNA

DSBs (Menke et al., 2001; Hryciw et al., 2002). In addition, MMS is an alkylating agent that is referred to commonly as radiomimetic (Xiao et al., 1996; Tsubouchi and Ogawa, 2000). This is confirmed by the fact that mutations in genes that are essential for the repair of DNA DSBs also confer sensitivity to MMS (Prakash and Prakash, 1977; Tsubouchi and Ogawa, 2000; Morishita et al., 2002). In addition, MMS induces transcriptional responses that are comparable to ionizing radiation (Gasch et al., 2001). By contrast, UV-B radiation, which produces mainly pyrimidine dimers, had the same effect on wild-type and *atm-1* plants. Interestingly, ATM deficiency in mammals also confers hypersensitivity to ionizing radiation but not to UV-B light, and the kinase activity of ATM is induced by radiation treatment (Banin et al., 1998; Canman et al., 1998). By contrast, yeast *mec1*, Drosophila *mei-41*, and mammalian cells expressing a mutant form of ATR are hypersensitive to both ionizing radiation and UV-B light (Cliby et al., 1998; Wright et al., 1998). These functional homologies between AtAtm and ATM, and between ATR, Mec1p, and Rad3, confirm our previous structural observations that AtAtm is more related to ATM than to ATR (Garcia et al., 2000).

AtAtm Is Essential for the Transcriptional Response to Ionizing Radiation

In contrast to the developmentally regulated transcription of meiosis-specific genes, the transcriptional induction of *AtRAD51*, *AtPARP1*, *ATGR1*, and *AtLIG4* by ionizing radiation was severely compromised in *atm-1* and *atm-2* mutants. This fact suggests that AtAtm plays a crucial role in the signaling that leads to the transcriptional response to ionizing radiation but not during meiosis. Our results also show that in the wild type, the induction is rapid—within 1 h—and transient. The peak of induction of *AtRAD51*, *AtPARP1*, and *ATGR1* was reached within 1 to 2 h after irradiation. At 6 h after irradiation, the levels still were higher than those in the control, but they were well below the peak value. It should be noted that, in contrast to mammalian cells, where the regulation of RAD51 is post-transcriptional and correlated with the formation of foci (Raderschall et al., 1999), plants use another level of regulation. It is currently not known whether post-transcriptional regulation of AtRad51 subcellular distribution occurs in plants. In yeast, Mec1p is known to control the expression of several genes in response to DNA damage (Gasch et al., 2001). Yeast *RAD51* transcription also is induced by ionizing radiation, and this induction depends on Mec1p (Gasch et al., 2001). Thus, the transcriptional level of regulation after ionizing radiation treatment and its control by homologs of ATM seem to be conserved between plants and yeast. The absence of the transcriptional induction of genes implicated in the repair of DSBs by homologous recombination (*AtRAD51*) or NHEJ (*AtLIG4*) also could provide a basis for the radiation sensitivity of *atm* mutants. This could be attributable to lower levels or an insufficient turnover of DSB repair activities. Whether the lack of NHEJ or HR activities or both is responsible for this sensitivity is unknown, and further studies will be required to answer this question.

In conclusion, Arabidopsis AtAtm plays a central role in the perception and response to DNA damage. The Arabidopsis *atm* mutants do not display major growth defects, in contrast to mutants in ATM homologs from other organisms, including humans. This study explores the role of AtAtm in meiosis and in the global response to ionizing radiation. Because mammalian Atm is involved in many aspects of cellular homeostasis, further studies will be necessary to fully explore the function of AtAtm in Arabidopsis. In particular, telomere metabolism, cell cycle control, and the regulation of transcription and recombination will be worth pursuing. Finally, the potential dual role of AtAtm in cell cycle control and the repair of DSBs opens new perspectives for both the control of plant growth in adverse environmental conditions and more precise plant genome manipulation by homologous recombination.

METHODS

Plant Material, Growth Conditions, and Mutant Screening

Arabidopsis plants were cultivated in a growth chamber with a 14-h photoperiod cycle on Seedlingsubstrat (Klasmann-Deilmann, Geeste, Germany). Lighting was provided by Powerstar HQI-BT 400/D lamps (Osram, Munich, Germany). The light intensity was 250 $\mu mol \cdot m^{-2} \cdot s^{-1}$. Temperature was set at 21°C during the light period and 18°C during the dark period. In vitro–grown plants were cultivated on germination medium [10 g/L Glc, 8 g/L Bacto-agar (Difco), 5 mM KNO_3, 2.5 mM KPO_4, 2 mM $MgSO_4$, 2 mM $Ca(NO_3)_2$, 2 mM microelements (Santoni et al., 1994), pH 5.5, supplemented with 0.01% Fe-citrate after autoclaving] on sterile Petri plates. The in vitro growth conditions were 14 h of light, provided by ColdWhite and Fluora lamps (Osram), at 75 $\mu mol \cdot m^{-2} \cdot s^{-1}$, and 8 h of darkness, with the temperature set at 21°C during the light cycle and 18°C during the dark cycle. For growth on germination medium, seeds were surface-sterilized in a sodium hypochlorite:ethanol:Tween solution (1 mL of sodium hypochlorite solution, 9 mL of ethanol, and two drops of Tween 20) and rinsed twice in ethanol. The sodium hypochlorite solution was prepared with one tablet of 44.4% sodium hypochlorite (Avix, Mourrière les Avignons, France) dissolved in 40 mL of water.

The collection of T-DNA mutants screened for an insertion in *AtATM* was generated in the Wassilewskija ecotype at the Institut National de la Recherche Agronomique (Bechtold et al., 1993; Bouchez and Hofte, 1998). A total of 36,864 genomic DNA extracts from T-DNA–mutagenized lines, grouped in 48 hyperpools, were tested by PCR as described by Geelen et al. (2000), with a combination of 20 *AtATM* primers (their sequences are available from the authors upon request) and 4 T-DNA–specific primers to cover the *AtATM* locus. PCR conditions were the same for all of the primer combinations, as follows: 94°C for 2 min, followed by 10 cycles with a decrease in annealing temperature (94°C for 15 s, 65 to 0.5°C per cycle for 15 s, and 68°C for 2 min), followed by 35 cycles (94°C for 15 s, 60°C for 15 s, and 68°C for 2 min) in the presence of 2 units of a Taq

(Sigma)/Pwo (Roche, Indianapolis, IN) polymerases (100:1) enzymatic mix.

The *atm-2* mutation was found in the searchable database of T-DNA insertion sequences established by the Salk Institute Genome Analysis Laboratory. The T-DNA Express database is accessible at http://signal.salk.edu/cgi-bin/tdnaexpress. DNA flanking the left border of the T-DNA was amplified with the T-DNA primers recommended by the Salk Institute Genome Analysis Laboratory and sequenced. No amplification could be achieved from the right border, suggesting that the right side of the T-DNA is truncated.

For segregation analysis and for the selection of plants homozygous or heterozygous for the T-DNA insertion, germination medium was supplemented with 5 μg/mL 5-phosphinotricine (Sigma), or seedlings on compost were sprayed with 1 mL/L Basta herbicide (AgrEvo France, Gif-sur-Yvette, France).

Sequencing of T-DNA Insertion Sites

For the *atm-1* insertion, the following primer combinations were used to amplify DNA flanking the T-DNA. At the right border, TAG3 (5′-CTGATACCAGACGTTGCCCGCATAA-3′) and ATM123 (5′-ATGAACTTGGAAGGGTTACAAGA-3′), and at the left border, TAG6 (5′-CACTCAGTCTTTCATCTACGGCA-3′) and ATM104 (5′-TGGCAGCCGAGTATTTTTCAACTTT-3′). For the *atm-2* mutation, the left border–flanking DNA was amplified with LBa1 (5′-GCGTGGACCGCTTGCTGCAACT-3′) and ATM126 (5′-TCTCTCCTTGTTTCAAGCTCTGC-3′). The DNA flanking the right border could not be amplified with primers located on the T-DNA. To circumvent this problem, flanking DNA was amplified by inverse PCR, as described by Thomas et al. (1994). The DNA was digested by PstI, and the primers used for amplification were ATM138 (5′-AATTGGCATCGGACTTGCTA-3′) and ATM140 (5′-GCAACCCAAAACAGGAAAA-3′).

The PCR products then were sequenced using one of the amplifying primers supplied with the BigDye terminator kit (PE–Applied Biosystems) and analyzed on an ABI Prism 310 sequencing machine (PE–Applied Biosystems).

RNA Gel Blot Analysis

Total RNA was prepared from homozygous and *atm* seedlings as described by Kloppstech et al. (1991). Twenty micrograms of total RNA then was loaded and separated on a 1% agarose gel and transferred to a nylon membrane according to standard procedures (Sambrook et al., 1989). cDNA fragments from the genes tested (*AtRAD51*, *AtPARP1*, *AtGR1*, and *AtLIG4*) were ^{32}P labeled with the Megaprime labeling kit (Amersham Biosciences) according to the manufacturer's instructions and hybridized to the membranes as described by Church and Gilbert (1984).

Quantification of Transcripts by Real-Time Reverse Transcriptase–Mediated PCR

Total RNA was extracted from inflorescences or 5-day-old seedlings with TRIzol (Invitrogen SARL, Cergy Pontoise, France) according to the manufacturer's instructions. To increase the proportion of meiotic tissues in the inflorescence, flower buds beyond stages 11 to 12 were removed manually. The flower stages correspond to those described by Bowman et al. (1991). One microgram of total RNA then was reverse-transcribed with the First-Strand cDNA Synthesis Kit (Amersham Biosciences Europe) using random hexamers as primers. The resulting cDNA was diluted 50-fold, and 1 μL was used in the quantitative amplification reaction for the sample genes (*AtRAD51*, *AtSPO11*, and *AtDMC1*). Amplification was performed in a volume of 25 μL with the Platinum Quantitative PCR Supermix-UDG (Invitrogen SARL), SYBRGreen, and the following primers: AtRAD51forward (5′-CGAGGAAGGATCTCTTGCAG-3′), AtRAD51reverse (5′-GCACTAGTGAACCCCAGAGG-3′), AtDMC1forward (5′-TTGTTCAGGAAAGGCAAAGG-3′), AtDMC1reverse (5′-GCTTCAGCTTCAGCGAGATT-3′), AtSPO11-1forward (5′-TCAGGAGTCGCAAGAACCTT-3′), and ATSPO11-1reverse (5′-ACGAACCGCTGCATTGTTAT-3′). As a reference, the 18S RNA gene was used in identical conditions except that the cDNA was diluted an additional 25-fold with the following primers: 18Sforward (5′-CGGCTACCACATCCAAGGAA-3′) and 18Sreverse (5′-GCTGGAATTACCGCGGCT-3′). Each sample was assayed in triplicate, and each experiment (i.e., from RNA extraction to quantification) was performed twice independently. To compare the transcript levels between the wild-type and mutant samples, the calculations were performed as follows. First, the difference in the cycle threshold (Ct) values between the 18S gene and a sample gene was calculated ($\Delta Ct_{gene\text{-}18S}$). Then, the difference between these values for wild-type and *atm* samples was calculated as follows: $\Delta Ct_{wt\text{-}atm} = (\Delta Ct_{gene\text{-}18S})_{wt} - (\Delta Ct_{gene\text{-}18S})_{atm}$. Finally, to determine the ratio of expression levels in *atm* versus wild-type plants for a given gene, that difference was increased to a power of 2: $atm/wt = 2^{\Delta Ctwt\text{-}atm}$.

AtATM Antibody Production and Protein Gel Blot Analysis

An *AtATM* cDNA fragment corresponding to the 202 C-terminal amino acids was cloned into pQE31 (Qiagen, Valencia, CA) to generate a 6× His-tag fusion peptide. This fusion peptide was purified on a nickel-agarose column and used to raise rabbit polyclonal antibodies.

For AtAtm expression analysis, calli and 10-day-old seedling extracts were prepared. One gram of fresh seedlings and 2 g of calli were ground on ice in the following buffer: 0.1 M sodium phosphate, pH 7, 1 M DTT, 2% polyvinylpolypyrrolidone, and antiproteases (Complete Inhibitor Cocktail; Roche). The slurry then was centrifuged to remove the debris, and the supernatant was recovered and used for subsequent analysis. Equal amounts of proteins were loaded onto a 5% SDS–polyacrylamide gel for electrophoresis according to Laemmli (1970) on a Mini-Protean apparatus (Bio-Rad). After electrophoresis, the proteins were electroblotted to a nitrocellulose membrane in the following buffer: 25 mM Tris, 192 mM Gly, 1% methanol, and 0.01% SDS. The protein gel blots then were probed with the anti-AtAtm serum (1:500 dilution) and revealed with the enhanced chemiluminescence kit (Roche).

γ-Rays, Methylmethane Sulfonate, and UV-B Sensitivity Tests

Five-day-old seedlings on sterile germination medium were γ-irradiated with doses ranging from 0 to 200 Gy, using a ^{60}Co source at a dose rate of 25 Gy/min. For global sensitivity analysis, plants were returned to the growth chamber and sensitivity was assayed after 21 days. For root growth sensitivity, germination plates were placed in a vertical position, irradiated after 5 days, and then put back into the

growth chamber. Root length was measured every day after irradiation. The same procedure was performed to test UV-B sensitivity (310 nm). UV-B radiation was provided by a UV light (Bioblock Scientific, Illkirch, France), with a flux rate of 2.5 mW/cm^2, and irradiation was given at doses up to 1 J/cm^2. After irradiation, the plates were transferred for 24 h into the dark and then returned to normal growing conditions.

For methylmethane sulfonate sensitivity tests, 5-day-old seedlings were placed in liquid germination medium (as described above but without Phytagel) supplemented with up to 100 ppm of methylmethane sulfonate (Fluka) and incubated for 15 days on an orbital shaker at 100 rpm under constant illumination.

Light and Confocal Microscopy

Mature pollen grain viability was assayed according to Alexander (1969). Observations were made with a light microscope (Dialux 20; Leitz, Wetzlar, Germany), and photographs were taken using Kodak film.

The development of female gametophytes was observed by confocal laser scanning microscopy. The 543-nm laser line and a 560- to 615-nm emission filter set were used (Axiovert 100M, equipped with a He/Ne laser; Zeiss, Jena, Germany) after coloration, as described by Christensen et al. (1996).

For the observation of meiosis, young anthers were prepared and DNA was stained with 4′,6-diamidino-2-phenylindole, according to Ross et al. (1996).

Meiotic Recombination Assay

The following marker lines obtained from the Nottingham Arabidopsis Stock Center were crossed with plants homozygous for the T-DNA insertion at the *AtATM* locus. Line NW4 contains the *ch1-1* and *gl2-1* mutations on chromosome 1, resulting in green-yellow leaves (*ch1-1*) without trichomes (*gl2-1*). NW9 contains the *ttg-1 yi-1* mutations on chromosome 5, resulting in no trichomes on stems and leaves (*ttg-1*), yellowish flower buds, and yellowish sharper leaves (*yi-1*).

Upon request, all novel materials described in this article will be made available in a timely manner for noncommercial research purposes.

Accession Number

The accession number for BAC T24C20 is AL096856.

ACKNOWLEDGMENTS

We thank Cliff Bray for providing the *AtLIG4* cDNA clone, Michael Kazmaier for providing the *ATGR1* and *AtPARP1* cDNA clones, Jean-Emmanuel Faure for help with the cytology of Arabidopsis female gametophytes, and Marie-Pascale Doutriaux, Christophe de la Roche Saint-André, and Christian Triantaphylidès for critical reading of the manuscript. We thank the Salk Institute Genomic Analysis Laboratory for providing the sequence-indexed Arabidopsis T-DNA insertion mutants. V.G. was supported by a predoctoral fellowship (Contrat Formation Recherche) from the Commissariat à l'Energie Atomique.

Received July 26, 2002; accepted October 25, 2002.

REFERENCES

Alexander, M.P. (1969). Differential staining of aborted and nonaborted pollen. Stain Technol. **44,** 117–122.

Andegeko, Y., Moyal, L., Mitelman, L., Tsarfaty, I., Shiloh, Y., and Rotman, G. (2001). Nuclear retention of ATM at sites of DNA double strand breaks. J. Biol. Chem. **276,** 38224–38230.

Angelis, K.J., McGuffie, M., Menke, M., and Schubert, I. (2000). Adaptation to alkylation damage in DNA measured by the comet assay. Environ. Mol. Mutagen. **36,** 146–150.

Banin, S., Moyal, L., Shieh, S., Taya, Y., Anderson, C.W., Chessa, L., Smorodinsky, N.I., Prives, C., Reiss, Y., Shiloh, Y., and Ziv, Y. (1998). Enhanced phosphorylation of p53 by ATM in response to DNA damage. Science **281,** 1674–1677.

Barlow, C., Liyanage, M., Moens, P.B., Deng, C.X., Ried, T., and Wynshaw-Boris, A. (1997). Partial rescue of the prophase I defects of Atm-deficient mice by p53 and p21 null alleles. Nat. Genet **17,** 462–466.

Barlow, C., Liyanage, M., Moens, P.B., Tarsounas, M., Nagashima, K., Brown, K., Rottinghaus, S., Jackson, S.P., Tagle, D., Ried, T., and Wynshaw-Boris, A. (1998). Atm deficiency results in severe meiotic disruption as early as leptonema of prophase I. Development **125,** 4007–4017.

Baskaran, R., Wood, L.D., Whitaker, L.L., Canman, C.E., Morgan, S.E., Xu, Y., Barlow, C., Baltimore, D., Wynshaw-Boris, A., Kastan, M.B., and Wang, J.Y. (1997). Ataxia telangiectasia mutant protein activates c-Abl tyrosine kinase in response to ionizing radiation. Nature **387,** 516–519.

Bechtold, N., Ellis, J., and Pelletier, G. (1993). *In planta Agrobacterium*-mediated gene transfer by infiltration of adult *Arabidopsis thaliana* plants. C. R. Acad. Sci. Paris **316,** 1194–1199.

Bishop, D.K., Park, D., Xu, L., and Kleckner, N. (1992). DMC1: A meiosis-specific yeast homolog of *E. coli* recA required for recombination, synaptonemal complex formation, and cell cycle progression. Cell **69,** 439–456.

Blanc, G., Barakat, A., Guyot, R., Cooke, R., and Delseny, M. (2000). Extensive duplication and reshuffling in the Arabidopsis genome. Plant Cell **12,** 1093–1102.

Bosotti, R., Isacchi, A., and Sonnhammer, E.L. (2000). FAT: A novel domain in PIK-related kinases. Trends Biochem. Sci. **25,** 225–227.

Bouchez, D., and Hofte, H. (1998). Functional genomics in plants. Plant Physiol. **118,** 725–732.

Bowman, J.L., Drews, G.N., and Meyerowitz, E.M. (1991). Expression of the Arabidopsis floral homeotic gene AGAMOUS is restricted to specific cell types late in flower development. Plant Cell **3,** 749–758.

Canman, C.E., Lim, D.S., Cimprich, K.A., Taya, Y., Tamai, K., Sakaguchi, K., Appella, E., Kastan, M.B., and Siliciano, J.D. (1998). Activation of the ATM kinase by ionizing radiation and phosphorylation of p53. Science **281,** 1677–1679.

Carpenter, A.T. (1979). Recombination nodules and synaptonemal complex in recombination-defective females of *Drosophila melanogaster*. Chromosoma **75,** 259–292.

Chlebowicz, E., and Jachymczyk, W.J. (1979). Repair of MMS-induced DNA double-strand breaks in haploid cells of *Saccharomyces cerevisiae*, which requires the presence of a duplicate genome. Mol. Gen. Genet. **167,** 279–286.

Christensen, C.A., King, E.J., Jordan, J.R., and Drews, G.N. (1996). Megagametogenesis in Arabidopsis wild-type and the Gf mutant. Sex. Plant Reprod. **10,** 49–64.

Church, G.M., and Gilbert, W. (1984). Genomic sequencing. Proc. Natl. Acad. Sci. USA **81,** 1991–1995.

Cliby, W.A., Roberts, C.J., Cimprich, K.A., Stringer, C.M., Lamb, J.R., Schreiber, S.L., and Friend, S.H. (1998). Overexpression of a kinase-inactive ATR protein causes sensitivity to DNA-damaging agents and defects in cell cycle checkpoints. EMBO J. **17,** 159–169.

Cortez, D., Wang, Y., Qin, J., and Elledge, S.J. (1999). Requirement of ATM-dependent phosphorylation of brca1 in the DNA damage response to double-strand breaks. Science **286,** 1162–1166.

Couteau, F., Belzile, F., Horlow, C., Grandjean, O., Vezon, D., and Doutriaux, M.P. (1999). Random chromosome segregation without meiotic arrest in both male and female meiocytes of a dmc1 mutant of Arabidopsis. Plant Cell **11,** 1623–1634.

Deveaux, Y., Alonso, B., Pierrugues, O., Godon, C., and Kazmaier, M. (2000). Molecular cloning and developmental expression of AtGR1, a new growth-related Arabidopsis gene strongly induced by ionizing radiation. Radiat. Res. **154,** 355–364.

Doucet-Chabeaud, G., Godon, C., Brutesco, C., de Murcia, G., and Kazmaier, M. (2001). Ionising radiation induces the expression of PARP-1 and PARP-2 genes in Arabidopsis. Mol. Genet. Genomics **265,** 954–963.

Garcia, V., Salanoubat, M., Choisne, N., and Tissier, A. (2000). An ATM homologue from *Arabidopsis thaliana*: Complete genomic organisation and expression analysis. Nucleic Acids Res. **28,** 1692–1699.

Gasch, A.P., Huang, M., Metzner, S., Botstein, D., Elledge, S.J., and Brown, P.O. (2001). Genomic expression responses to DNA-damaging agents and the regulatory role of the yeast atr homolog mec1p. Mol. Biol. Cell **12,** 2987–3003.

Gatei, M., Young, D., Cerosaletti, K.M., Desai-Mehta, A., Spring, K., Kozlov, S., Lavin, M.F., Gatti, R.A., Concannon, P., and Khanna, K. (2000). ATM-dependent phosphorylation of nibrin in response to radiation exposure. Nat. Genet. **25,** 115–119.

Geelen, D., Lurin, C., Bouchez, D., Frachisse, J.M., Lelievre, F., Courtial, B., Barbier-Brygoo, H., and Maurel, C. (2000). Disruption of putative anion channel gene AtCLC-a in Arabidopsis suggests a role in the regulation of nitrate content. Plant J. **21,** 259–267.

Herceg, Z., and Wang, Z.Q. (2001). Functions of poly(ADP-ribose) polymerase (PARP) in DNA repair, genomic integrity and cell death. Mutat. Res. **477,** 97–110.

Hryciw, T., Tang, M., Fontanie, T., and Xiao, W. (2002). MMS1 protects against replication-dependent DNA damage in *Saccharomyces cerevisiae*. Mol. Genet. Genomics **266,** 848–857.

Jongmans, W., Vuillaume, M., Chrzanowska, K., Smeets, D., Sperling, K., and Hall, J. (1997). Nijmegen breakage syndrome cells fail to induce the p53-mediated DNA damage response following exposure to ionizing radiation. Mol. Cell. Biol. **17,** 5016–5022.

Karran, P. (2000). DNA double strand break repair in mammalian cells. Curr. Opin. Genet. Dev. **10,** 144–150.

Kastan, M.B., and Lim, D.S. (2000). The many substrates and functions of ATM. Nat. Rev. Mol. Cell Biol. **1,** 179–186.

Kato, R., and Ogawa, H. (1994). An essential gene, ESR1, is required for mitotic cell growth, DNA repair and meiotic recombination in *Saccharomyces cerevisiae*. Nucleic Acids Res. **22,** 3104–3112.

Khanna, K.K., and Jackson, S.P. (2001). DNA double-strand breaks: Signaling, repair and the cancer connection. Nat. Genet **27,** 247–254.

Kim, S.T., Lim, D.S., Canman, C.E., and Kastan, M.B. (1999). Substrate specificities and identification of putative substrates of ATM kinase family members. J. Biol. Chem. **274,** 37538–37543.

Klimyuk, V.I., and Jones, J.D. (1997). AtDMC1, the Arabidopsis homologue of the yeast DMC1 gene: Characterization, transposon-induced allelic variation and meiosis-associated expression. Plant J. **11,** 1–14.

Kloppstech, K., Otto, B., and Sierralta, W. (1991). Cyclic temperature treatments of dark-grown pea seedlings induce a rise in specific transcript levels of light-regulated genes related to photomorphogenesis. Mol. Gen. Genet. **225,** 468–473.

Laemmli, U.K. (1970). Cleavage of structural proteins during the assembly of the head of bacteriophage T4. Nature **227,** 680–685.

Li, S., Ting, N.S., Zheng, L., Chen, P.L., Ziv, Y., Shiloh, Y., Lee, E.Y., and Lee, W.H. (2000). Functional link of BRCA1 and ataxia telangiectasia gene product in DNA damage response. Nature **406,** 210–215.

Lydall, D., Nikolsky, Y., Bishop, D.K., and Weinert, T. (1996). A meiotic recombination checkpoint controlled by mitotic checkpoint genes. Nature **383,** 840–843.

Lydall, D., and Weinert, T. (1995). Yeast checkpoint genes in DNA damage processing: Implications for repair and arrest. Science **270,** 1488–1491.

Masson, J.E., King, P.J., and Paszkowski, J. (1997). Mutants of *Arabidopsis thaliana* hypersensitive to DNA-damaging treatments. Genetics **146,** 401–407.

Masson, J.E., and Paszkowski, J. (1997). *Arabidopsis thaliana* mutants altered in homologous recombination. Proc. Natl. Acad. Sci. USA **94,** 11731–11735.

Menke, M., Chen, I., Angelis, K.J., and Schubert, I. (2001). DNA damage and repair in *Arabidopsis thaliana* as measured by the comet assay after treatment with different classes of genotoxins. Mutat. Res. **493,** 87–93.

Morishita, T., Tsutsui, Y., Iwasaki, H., and Shinagawa, H. (2002). The *Schizosaccharomyces pombe* rad60 gene is essential for repairing double-strand DNA breaks spontaneously occurring during replication and induced by DNA-damaging agents. Mol. Cell. Biol. **22,** 3537–3548.

Norbury, C.J., and Hickson, I.D. (2001). Cellular responses to DNA damage. Annu. Rev. Pharmacol. Toxicol. **41,** 367–401.

Prakash, L., and Prakash, S. (1977). Isolation and characterization of MMS-sensitive mutants of *Saccharomyces cerevisiae*. Genetics **86,** 33–55.

Raderschall, E., Golub, E.I., and Haaf, T. (1999). Nuclear foci of mammalian recombination proteins are located at single-stranded DNA regions formed after DNA damage. Proc. Natl. Acad. Sci. USA **96,** 1921–1926.

Ries, G., Heller, W., Puchta, H., Sandermann, H., Seidlitz, H.K., and Hohn, B. (2000). Elevated UV-B radiation reduces genome stability in plants. Nature **406,** 98–101.

Ross, K.J., Fransz, P., Armstrong, S.J., Vizir, I., Mulligan, B., Franklin, F.C., and Jones, G.H. (1997). Cytological characterization of four meiotic mutants of Arabidopsis isolated from T-DNA-transformed lines. Chromosome Res. **5,** 551–559.

Ross, K.J., Fransz, P., and Jones, G.H. (1996). A light microscopic atlas of meiosis in *Arabidopsis thaliana*. Chromosome Res. **4,** 507–516.

Rotman, G., and Shiloh, Y. (1998). ATM: From gene to function. Hum. Mol. Genet. **7,** 1555–1563.

Rozema, J., van de Staaij, J., Björn, L.O., and Caldwell, M.M.

(1997). UV-B as an environmental factor in plant life: Stress and regulation. Trends Ecol. Evol. **12,** 22–28.

Sambrook, J., Fritsch, E.F., and Maniatis, T. (1989). Molecular Cloning: A Laboratory Manual, 2nd ed. (Cold Spring Harbor, NY: Cold Spring Harbor Laboratory Press).

Santoni, V., Bellini, C., and Caboche, M. (1994). Use of two-dimensional protein-pattern analysis for the characterization of Arabidopsis mutants. Planta **192,** 557–566.

Savitsky, K., et al. (1995). A single ataxia telangiectasia gene with a product similar to PI-3 kinase. Science **268,** 1749–1753.

Schar, P., Herrmann, G., Daly, G., and Lindahl, T. (1997). A newly identified DNA ligase of *Saccharomyces cerevisiae* involved in RAD52-independent repair of DNA double-strand breaks. Genes Dev. **11,** 1912–1924.

Shafman, T., et al. (1997). Interaction between ATM protein and c-Abl in response to DNA. Nature **387,** 520–523.

Shinohara, A., Ogawa, H., and Ogawa, T. (1992). Rad51 protein involved in repair and recombination in *S. cerevisiae* is a RecA-like protein. Cell **69,** 457–470.

Smith, G.C., Cary, R.B., Lakin, N.D., Hann, B.C., Teo, S.H., Chen, D.J., and Jackson, S.P. (1999). Purification and DNA binding properties of the ataxia-telangiectasia gene product ATM. Proc. Natl. Acad. Sci. USA **96,** 11134–11139.

Teo, S.H., and Jackson, S.P. (1997). Identification of *Saccharomyces cerevisiae* DNA ligase IV: Involvement in DNA double-strand break repair. EMBO J. **16,** 4788–4795.

Thacker, J. (1999). Repair of ionizing radiation damage in mammalian cells: Alternative pathways and their fidelity. C. R. Acad. Sci. Ser. III Life Sci. **322,** 103–108.

Thomas, C.M., Jones, D.A., English, J.J., Carroll, B.J., Bennetzen, J.L., Harrison, K., Burbidge, A., Bishop, G.J., and Jones, J.D. (1994). Analysis of the chromosomal distribution of transposon-carrying T-DNAs in tomato using the inverse polymerase chain reaction. Mol. Gen. Genet. **242,** 573–585.

Tissier, A.F., Marillonnet, S., Klimyuk, V., Patel, K., Torres, M.A., Murphy, G., and Jones, J.D. (1999). Multiple independent defective suppressor-mutator transposon insertions in Arabidopsis: A tool for functional genomics. Plant Cell **11,** 1841–1852.

Tsubouchi, H., and Ogawa, H. (2000). Exo1 roles for repair of DNA double-strand breaks and meiotic crossing over in *Saccharomyces cerevisiae*. Mol. Biol. Cell **11,** 2221–2233.

Vision, T.J., Brown, D.G., and Tanksley, S.D. (2000). The origins of genomic duplications in Arabidopsis. Science **290,** 2114–2117.

Weinert, T. (1997). Yeast checkpoint controls and relevance to cancer. Cancer Surv. **29,** 109–132.

West, C.E., Waterworth, W.M., Jiang, Q., and Bray, C.M. (2000). Arabidopsis DNA ligase IV is induced by gamma-irradiation and interacts with an Arabidopsis homologue of the double strand break repair protein XRCC4. Plant J. **24,** 67–78.

Wilson, T.E., Grawunder, U., and Lieber, M.R. (1997). Yeast DNA ligase IV mediates non-homologous DNA end joining. Nature **388,** 495–498.

Wong, A.K., et al. (1998). Characterization of a carboxy-terminal BRCA1 interacting protein. Oncogene **17,** 2279–2285.

Wright, J.A., Keegan, K.S., Herendeen, D.R., Bentley, N.J., Carr, A.M., Hoekstra, M.F., and Concannon, P. (1998). Protein kinase mutants of human ATR increase sensitivity to UV and ionizing radiation and abrogate cell cycle checkpoint control. Proc. Natl. Acad. Sci. USA **95,** 7445–7450.

Xiao, W., Chow, B.L., and Rathgeber, L. (1996). The repair of DNA methylation damage in *Saccharomyces cerevisiae*. Curr. Genet. **30,** 461–468.

Xu, Y., and Baltimore, D. (1996). Dual roles of ATM in the cellular response to radiation and in cell growth control. Genes Dev. **10,** 2401–2410.

Zhou, B.B., and Elledge, S.J. (2000). The DNA damage response: Putting checkpoints in perspective. Nature **408,** 433–439.